Impact of monsoon circulations on the upper troposphere and lower stratosphere

Andrew Gettelman and Douglas E. Kinnison

National Center for Atmospheric Research, Boulder, Colorado, USA

Timothy J. Dunkerton

Northwest Research Associates, Bellevue, Washington, USA

Guy P. Brasseur

National Center for Atmospheric Research, Boulder, Colorado, USA

Max Plank Institute for Meteorology, Hamburg, Germany

[1]   Observations from in situ aircraft and output from a global chemical transport model are used to better understand the impact of Northern Hemisphere summer monsoon circulations on stratosphere-troposphere exchange. A long-term model climatology resembles the satellite climatology of water vapor and ozone in the monsoon regions. A simulation with observed winds is able to reproduce individual transport events observed from aircraft, and these events are used to infer that large-scale motions and monsoon circulations can explain the global correlations of ozone and water vapor around the tropopause. A detailed analysis of model fluxes of water vapor and ozone indicates that the Asian monsoon circulation may contribute 75% of the total net upward water vapor flux in the tropics at tropopause levels from July to September. Some of this air may enter the tropical stratosphere and bypass the tropical tropopause altogether.   *INDEX TERMS:* 0341 Atmospheric Composition and Structure: Middle atmosphere—constituent transport and chemistry (3334); 3319 Meteorology and Atmospheric Dynamics: General circulation; 3374 Meteorology and Atmospheric Dynamics: Tropical meteorology; 3362 Meteorology and Atmospheric Dynamics: Stratosphere/troposphere interactions; *KEYWORDS:* monsoon, stratosphere, ozone

1. Introduction

[2]   Monsoon circulations, particularly those in Northern Hemisphere (boreal) summer, strongly affect the general circulation [*Webster et al.*, 1998]. The "monsoons" are continental- and seasonal-scale sea breeze circulations. The south Asian and North American summer monsoons are deep circulations, with closed anticyclones extending up to at least 70 hPa in the stratosphere in July and perhaps higher [*Dunkerton*, 1995]. The two monsoon circulations are different in magnitude, horizontal extent and depth, but similar in their forcing (a high-altitude land mass of the Himalayan or Colorado plateau to the north, and warm ocean regions of the Bay of Bengal or the Gulf of Mexico to the south). These deep circulations may have a significant impact on stratosphere-troposphere exchange, and on the entry of air into the stratosphere.

[3]   Because the annual cycle of tropopause layer temperatures is warmer in Northern Hemisphere summer than winter [*Yulaeva et al.*, 1994], most recent work has been focused on understanding tropical stratosphere-troposphere exchange in Northern Hemisphere winter, when temperatures are cold [*Randel et al.*, 2004]. However, *Smith et al.* [2000] recently noted that observed trends in water vapor in the lower stratosphere during the mid-1990s differ seasonally, and that water vapor changes were most positive in Northern Hemisphere fall. This highlights the importance of the boreal summer and fall seasons for understanding water vapor trends in the lower stratosphere.

[4]   The Asian and North American monsoons may have distinct effects on the upper troposphere and lower stratosphere. *Randel et al.* [2001] noted that while similarly high water vapor associated with both Asian and American monsoon circulations (~5 parts per million by volume or ppmv), ozone concentrations over the Indian subcontinent and Southeast Asia in July–September (~100 parts per billion by volume or ppbv) are far lower than over North America (~250 ppbv).

[5]   This study investigates the Northern Hemisphere summertime upper troposphere and lower stratosphere, in an attempt to better understand the impact of the monsoon circulations on the exchange of air between the troposphere and the stratosphere. A global chemical transport model

driven by observed winds is used, and described in section 2. The model distribution and transport of constituents is validated with in situ aircraft observations in the subtropics near the North American monsoon in section 3. Section 4 will extend this analysis using the global model to explain the observed correlations between ozone and water vapor in the monsoon regions and why they differ between the two major monsoon regions in Asia and North America. The model is also used in used in section 4 to illustrate that monsoon circulations may transport air directly from the troposphere into the tropical stratosphere, bypassing the tropical cold point tropopause. Conclusions are in section 5.

2. Methodology

2.1. Model

[6] In this study we use the Model for Ozone and Related Chemical Tracers, version 3 (MOZART3). This model is an extension of the tropospheric version of MOZART described by *Horowitz et al.* [2003]. The chemistry in the MOZART3 model includes the representation of 50 species important in the upper troposphere and lower stratosphere [*Park et al.*, 2004]. Surface boundary conditions for CH_4, N_2O, CO_2, CH_3Cl, CCl_4, CH_3CCH_3, $CFCl_3$, CF_2Cl_2, CFC-113, HCFC-22, CH_3Cl, CH_3Br, CF_3Br, and CF_2ClBr are based on observations. The model accounts for surface emissions of NO_x, and CO on the basis of the emission inventories described by *Horowitz et al.* [2003]. The NO_x source from lightning is distributed according to the location of convective clouds on the basis of *Price et al.* [1997] with a vertical profile following *Pickering et al.* [1998]. Aircraft emissions of NO_x and CO are included in the model on the basis of *Friedl* [1997]. A lightning source of nitrogen oxides keyed to convection, and climatological emissions from biomass burning, along with other surface source gas emissions are based on a climatology from *Horowitz et al.* [2003].

[7] The model uses the Model of Atmospheric Transport and Chemistry (MATCH) framework described by *Rasch et al.* [1997]. MATCH includes representations of advection, deep and shallow convection, boundary layer mixing, and wet and dry deposition. Advection of tracers is performed following *Lin and Rood* [1996]. Versions of the MOZART model have been recently used by *Park et al.* [2004] to analyze methane, water vapor and nitrogen oxides near the tropical tropopause, by *Horowitz et al.* [2003] to estimate global ozone fluxes and by *Sassi et al.* [2004] to understand the impact of El Niño on the middle atmosphere.

[8] The model is used in an off-line mode, driven by winds and temperatures from two different sources. The first source is output from a 22-year run of the National Center for Atmospheric Research (NCAR) Whole Atmosphere Community Climate Model version 1b (WACCM1b). WACCM1b is a general circulation model (GCM) with a fully resolved stratosphere. The run with GCM output uses observed sea surface temperatures and observed greenhouse source gases (i.e., CO_2, CH_4, N_2O, CFC-11, and CFC-12) for the period of 1979–2000. High-frequency (every 6 hours) meteorological output (e.g., U, V, T) is obtained from this simulation and used to drive the MOZART3 CTM. The MOZART3 CTM also is integrated over this period, trending the 14 long-lived gases (described above)

from observations. Surface source emissions of CO and NO_x are fixed climatologies. The second source of winds and temperatures to drive the MOZART CTM is analyses from the European Centre for Medium-Range Weather Forecasts (ECMWF) for the 2002 calendar year, with similar surface initializations.

[9] Model resolution for the ECMWF 2002 simulation is ~1.8 degrees in the horizontal and ~750 m vertically in the upper troposphere. For the climatological 22-year run, it is ~2.8 degrees in the horizontal and ~1100 m vertically in the upper troposphere.

2.2. Observations

[10] This study uses observations of water vapor and ozone from satellites for a global climatology. Water vapor data are from the Halogen Occultation Experiment (HALOE) on the Upper Atmosphere Research Satellite (UARS) from 1992 to 2002, based on the updated climatology described by *Randel et al.* [1999]. Ozone observations come from the Stratospheric Aerosol and Gas Experiment II (SAGE II) described by *McCormick et al.* [1989].
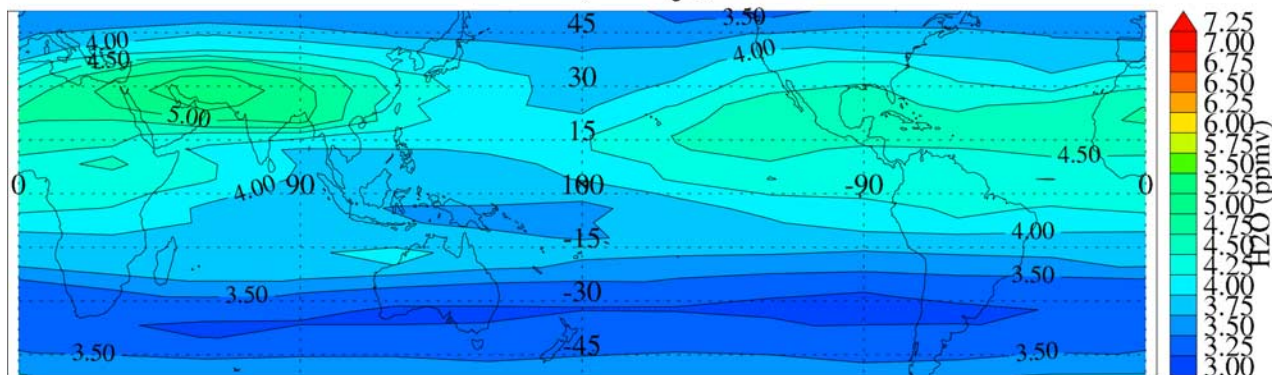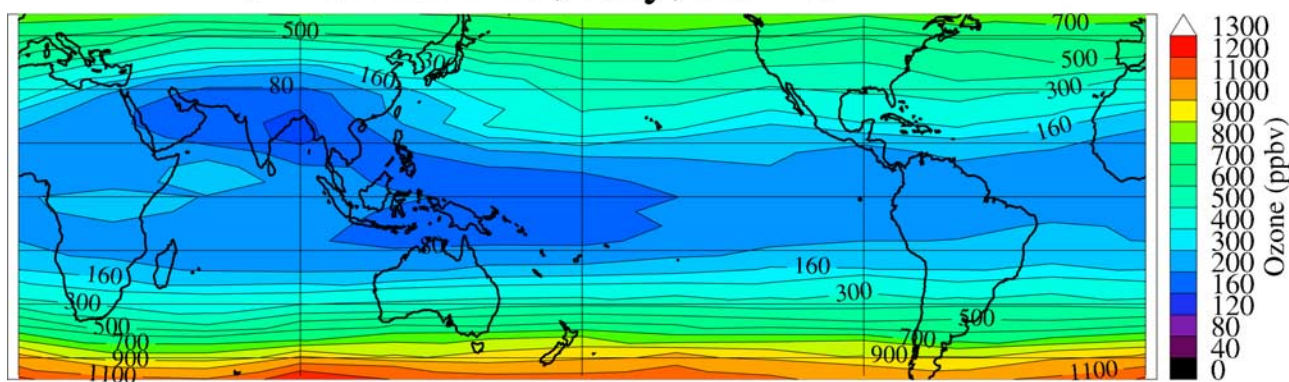
[11] In addition, a detailed and specific picture is provided by in situ aircraft observations of chemical tracers (chiefly water vapor and ozone) taken during the Cirrus Regional Study of Tropical Anvils and Cirrus Layers–Florida Area Cirrus Experiment (CRYSTAL-FACE) which took place over Florida in June–July 2002. Because our study is concentrated in the upper troposphere and lower stratosphere, data comes from the NASA WB57 aircraft which was tasked during the campaign with conducting in situ sampling in the upper troposphere and lower stratosphere. Measurements of ozone [*Proffitt and McLaughlin*, 1983], carbon monoxide [*Podolske and Loewenstein*, 1993] and water vapor [*Weinstock et al.*, 1994] are used in this study. More information is available from the CRYSTAL-FACE web site (http://cloud1.arc.nasa.gov/ crystalface/). In particular, we will focus on several different events during the mission, including anomalous ozone concentrations observed on 9 July 2002. The characteristics of this flight and others have been recently examined in detail by *Richard et al.* [2003] and *Ray et al.* [2004]. The model is used to extend the analysis performed by these authors.

3. Model Evaluation

[12] We begin with an analysis of observed and modeled climatology of ozone and water vapor for boreal summer, and then proceed on to a detailed analysis of specific transport events. First, we show maps of ozone and water vapor climatologies near 100 hPa from observations and the model.

3.1. Climatology

[13] Figure 1 illustrates a climatology of water vapor from HALOE at 100 hPa (Figure 1a) and ozone from SAGE at 95 hPa (Figure 1b). Water vapor (Figure 1a) peaks (~5.25 parts per million by volume or ppmv) just to the northwest of the Indian subcontinent near 30°N, and has a second smaller peak (~4.5 ppmv) centered over northern Mexico at 20°–30°N. These peaks are consistent with transport of tropospheric air with high water vapor to these

A) HALOE H2O, July, 100hPa

B) SAGE O3, July, 95hPa

Figure 1. Climatology of (a) water vapor from HALOE at 100 hPa and (b) ozone from SAGE at 95 hPa.

altitudes, and correspond with the Asian and American monsoon anticyclones respectively [*Dunkerton*, 1995]. The maxima are also clear in isentropic coordinates, extending further northward as the isentropes slope downward toward the poles (not shown). Water vapor has a minimum just south of the equator in the central and western Pacific, and again in the midlatitudes of the Southern Hemisphere.

[14] Ozone (Figure 1b), has a distinct minimum (<40 ppbv) over Nepal at 95 hPa. High water vapor and low ozone are consistent with transport of near surface air in deep convective systems. However, there is little evidence of any monsoon transport of low ozone values up to 95 hPa over North America. One hypothesis is that surface ozone is higher over North America than over Asia and therefore if convection is bringing large amounts of surface air into the upper troposphere and lower stratosphere, ozone will be higher over North America. However, mean ozone mixing ratios are generally greater than 200 parts per billion by volume (ppbv), much higher than near surface ozone.
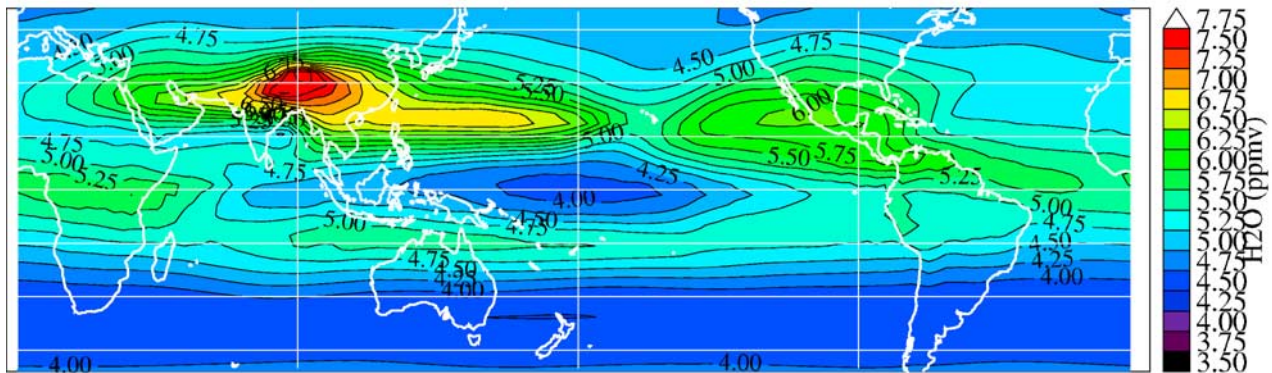
[15] These observations are compared to a climatology from the 22-year run of the MOZART CTM. Figure 2 presents water vapor (Figure 2a) and ozone (Figure 2b) mixing ratios on 100 hPa. Figure 2a illustrates that the model also produces two water vapor maxima over Asia and North America in July. The color scale for water vapor has been shifted by 0.5 ppmv relative to Figure 1a because the model is wetter than observations. Representative values of water vapor near the maxima are about 7.0 ppmv

(5.25 ppmv) for the model (observations) over Asia and 6 ppmv (4.5 ppmv) over North America. In both the model and observations, water vapor over south Asia is ~20% higher than over North America. A water vapor minimum below 4 ppmv is also found along the equator in central and western Pacific. Simulated ozone (Figure 2b) at 100 hPa also features low ozone over south Asia (<120 ppbv) and higher ozone (>200 ppbv) over North America. Both the model and observations produce an ozone minimum in the tropics south of the equator, and a planetary wave like structure with high ozone over the subtropical and midlatitude Pacific, and lower ozone over western North America. Ridging is more prominent in the model than observations.
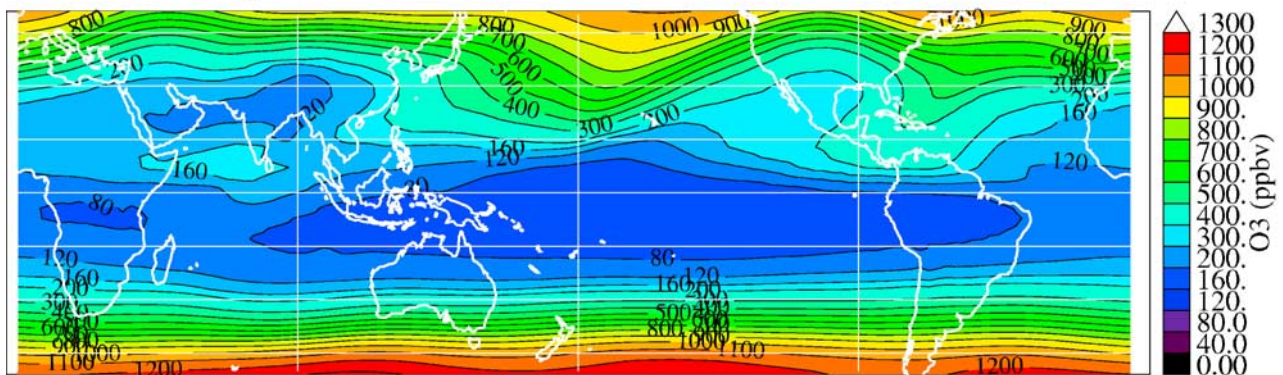
[16] The zonal mean climatological water vapor distribution in the stratosphere is examined at the end of the summer monsoon season (September) in Figure 3 for the 22-year MOZART model run (Figure 3a) and the observed HALOE climatology (Figure 3b). *Park et al.* [2004] have noted that the simulation used here has a reasonable annual cycle of water vapor in the lower stratosphere. In the model, there is a clear signature of high water vapor in the troposphere, with additional high water vapor amounts in the Northern Hemisphere reaching well up to 66 hPa, and of over 5 ppmv at the 400-K potential temperature surface. The situation is not as clear in the HALOE observations for September (Figure 3b). Observations show only slightly enhanced water vapor up to the 400-K potential temperature
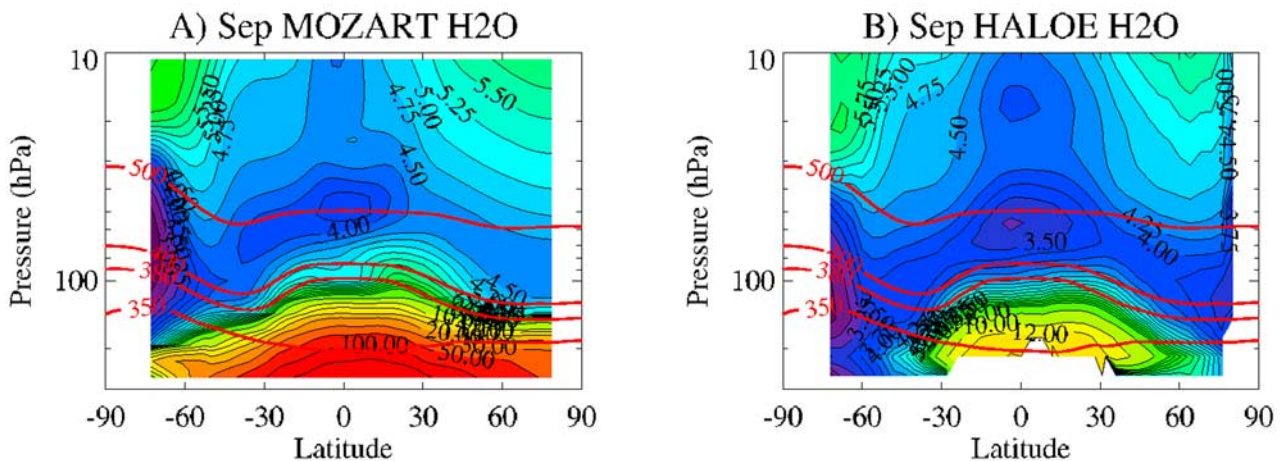
A) MOZART Jul H2O 100hPa
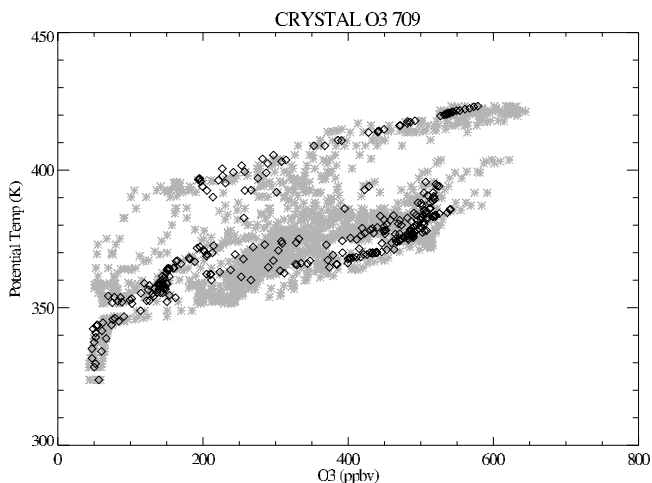

B) MOZART Jul O3 100hPa

Figure 2. Climatology of (a) water vapor and (b) ozone at 100 hPa from a 22-year MOZART simulation.

surface at 30°N. Regional averaged plots indicate that the strongest effect in both the simulation and observations is seen over the Asian monsoon. In the simulation, monthly mean plots indicate that the high values of water vapor populate the deep tropics in November and December, and water vapor concentrations at the tropical tropopause begin to drop in December. By this time the higher water vapor concentrations in the simulation are spread throughout the

Figure 3. Climatological zonal mean September water vapor (ppmv) for (a) MOZART 22-year simulation and (b) HALOE observations. Red lines indicate contours of potential temperature (350 K, 380 K, 400 K, and 500 K).

Figure 4. Ozone on the CRYSTAL-FACE flight track of 9 July 2002 as a function of potential temperature. Black diamonds, observations; grey asterisks, model-simulated ozone.

tropics, and the high water vapor propagates vertically. Some of the air appears to bypass the tropical tropopause entirely. Similar analysis of the HALOE climatology is not as clear regarding the source of the wet phase of the tape recorder and its propagation. Nonetheless, the fluxes from the model and the observations indicate an important role for the Asian monsoon in understanding the tropical "tape recorder" [*Mote et al.*, 1996] in stratospheric water vapor.

[17] One hypothesis is that water vapor transport occurs from the surface because of convection in both North America and south Asia. The Asian monsoon circulation is higher and deeper [*Dunkerton*, 1995]. The isolation of the south Asian monsoon anticyclone prevents mixing within the core of the monsoon at upper levels, leading to low ozone and high water vapor. Furthermore, over North America there is more significant mixing of convective air masses with stratospheric intrusions containing high ozone during local summer. The deeper circulation over Asia more strongly affects the stratosphere.
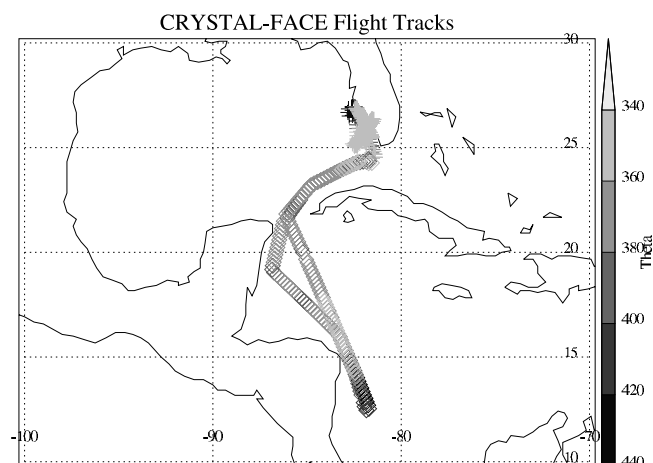
[18] In order to validate this hypothesis, particularly for the complex transport regime over North America, we will turn to a detailed analysis of a particular time period, when MOZART CTM simulations can be closely tied to observations. We show that in addition to the fidelity to the climatology illustrated for long-term runs in Figure 2, the CTM in a simulation driven with analyzed winds and temperatures can reproduce observations taken at specific locations and times. Then we can use the MOZART CTM to search for the sources of observed air, which helps to validate the hypothesis just presented.
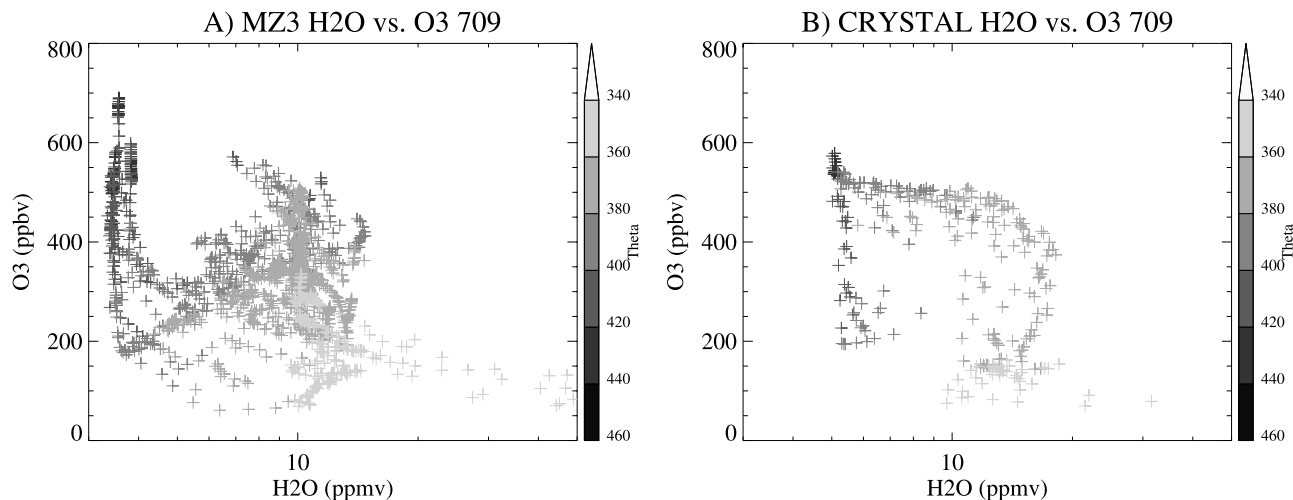
3.2. Specific Events

[19] For comparisons we focus on a particular day of observations during the CRYSTAL-FACE mission. *Richard et al.* [2003] have recently discussed the flow regime during July 2002 over eastern North America, and shown strong northerly flow from Canada down across the eastern United States. *Richard et al.* [2003] cite this as the reason for anomalous ozone "tongues" observed during CRYSTAL-

FACE. In Figure 4 we show the CRYSTAL-FACE observations of ozone from the flight on 9 July 2002, which originated out of Key West, Florida, and headed south (Figure 5). For comparison, ozone has also been interpolated from the MOZART simulation using ECMWF winds to the locations of the aircraft observations. To provide a better sampling of the model domain and an estimate of sensitivity to possible strong gradients, the model is sampled at 5 points; the observation location and 4 points ±4 degrees of latitude and longitude in each direction (∼2 model grid cells). In Figure 4, it is clear that the model is able to reproduce the basic large-scale structure of relatively high ozone over the Gulf of Mexico between the 350-K and 400-K isentropic surfaces. In particular, there is very good agreement between the simulation and observations in both the absolute value of ozone and its shape.

[20] A stricter test of the fidelity of the model simulation is its ability to reproduce tracer-tracer correlations. Figure 6 illustrates the observed water vapor and ozone correlations with the same correlations from the MOZART simulation, interpolated to the location of the observations (and local points around them). For ozone and water vapor, we expect different compact correlation relationships in the troposphere and stratosphere [*Ray et al.*, 2004]. In the stratosphere we expect ozone above 200 ppbv with low (<6 ppmv) water vapor, and increasing ozone with height. In the troposphere, we expect high water vapor, and low ozone (<100 ppbv). Such a situation exists for example, on air sampled over Florida on 21 July, illustrated in Figure 7 (the flight track for this flight is also illustrated in Figure 5). With the exception of low simulated water vapor for a portion of the track, the correspondence of the correlation curves between the model (Figure 7a) and observations (Figure 7b) is good. The situation on 9 July 2002 is more complex in both the model and observations (Figure 6). The ozone tongue is located between 350 K and 390 K with ozone values of 150–500 ppbv (Figure 4). These points have significantly higher water vapor than would be expected on the basis of their ozone concentration (or equivalently, higher ozone than expected on the basis of

Figure 5. Flight tracks of WB-57 for 9 July 2002 (diamonds) and 21 July 2002 (crosses). Shading indicates the potential temperature at each sampled point on the flight track.
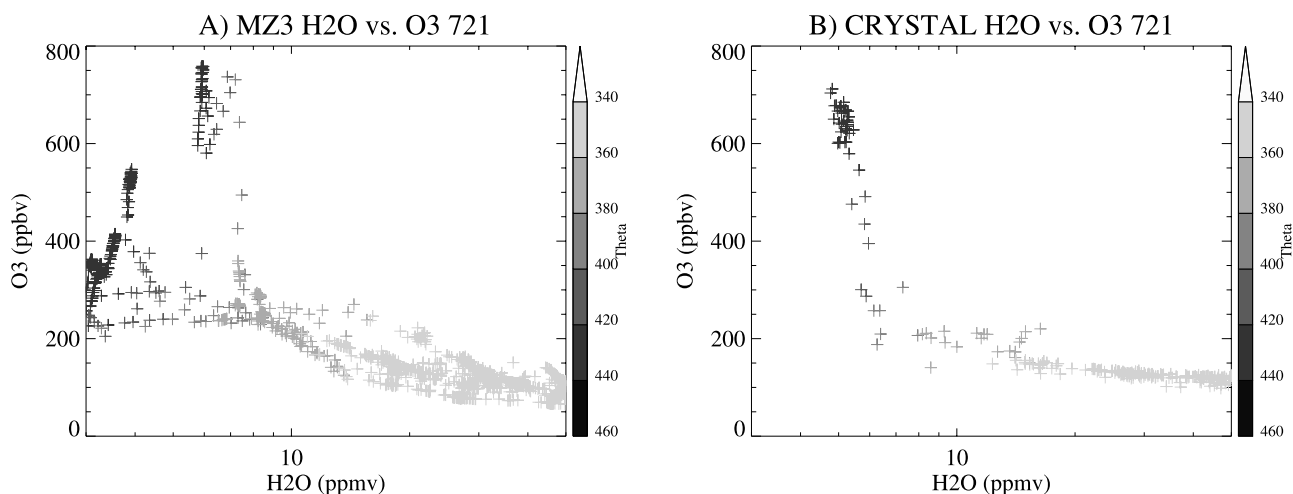
Figure 6. Correlations of ozone and water vapor on the CRYSTAL-FACE flight track of 9 July 2002 for (a) model simulation and (b) observations. Shading indicates the potential temperature at each point.

the water vapor concentration). If this is high-latitude air, as indicated by the meteorological situation [*Richard et al.*, 2003] and trajectory analysis [*Ray et al.*, 2004], then this air up to 380–390 K has higher water vapor than expected. We investigate the source of this water vapor below.

[21] Figure 8 illustrates the simulated water vapor and ozone fields at 113 hPa averaged for 9 July 2002. The 113-hPa surface is approximately the 380-K potential temperature surface. Here, high water vapor (up to 12 ppmv) is colocated with high ozone over Florida and the Gulf of Mexico. The high values extend off the Atlantic coast of North America. The high water vapor and ozone are located in the stratosphere, north of the tropopause, which is indicated in Figure 8 by the gray line as a contour of potential vorticity (2 PVU where 1 PVU ≡ 1 Kg^{-1} m^2 s^{-1}). The PV tropopause reveals a filament of tropical air (associated with a folded tropopause structure) in the eastern Pacific, extending onshore into the western United States,

and characterized by low ozone (<200 ppbv) and low water vapor.

[22] The origin of the high-ozone air on 9 July can be traced by following the structures back in time in the model. Daily maps such as those in Figure 8 show that high water vapor is injected into a stratospheric air mass over eastern Canada at 50°N, on 1–2 July. This injection is graphically illustrated by water vapor fluxes in Figure 9. In Figure 9a, the model net convective flux across 228 hPa (approximately the tropopause level at 50°N) is shown by latitude, averaged over North America. About 10 days prior to 9 July (indicated by the origin of the arrow in Figure 9), there is an upward convective flux of water vapor at 50°N, along with an additional vertical flux of water vapor from the model advection scheme (Figure 9b). This flux is also associated with southward meridional motion (Figure 9c). The upward water vapor flux can also be seen up to 95 hPa, with values of 10 ppmv at 95 hPa occurring at 50°N (not shown).
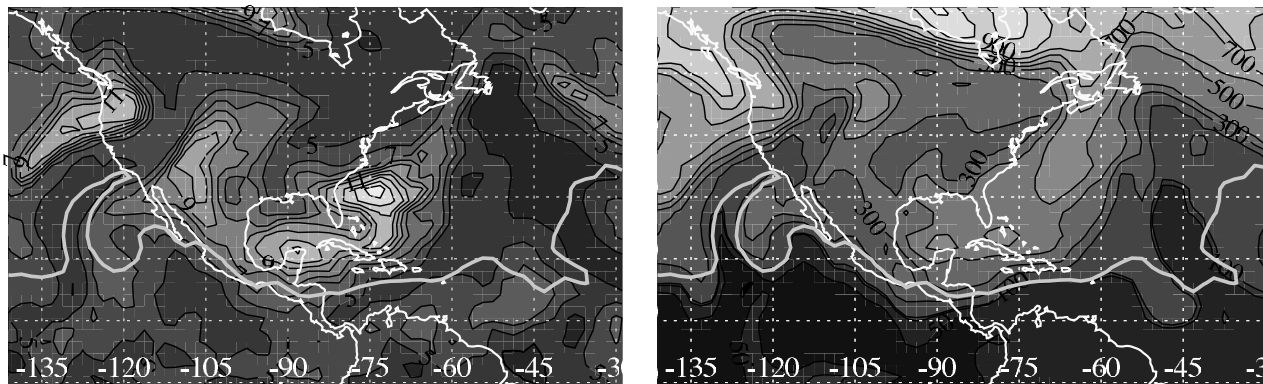

Figure 7. Correlations of ozone and water vapor on the CRYSTAL-FACE flight track of 21 July 2002 for (a) model simulation and (b) observations. Shading indicates the potential temperature at each point.
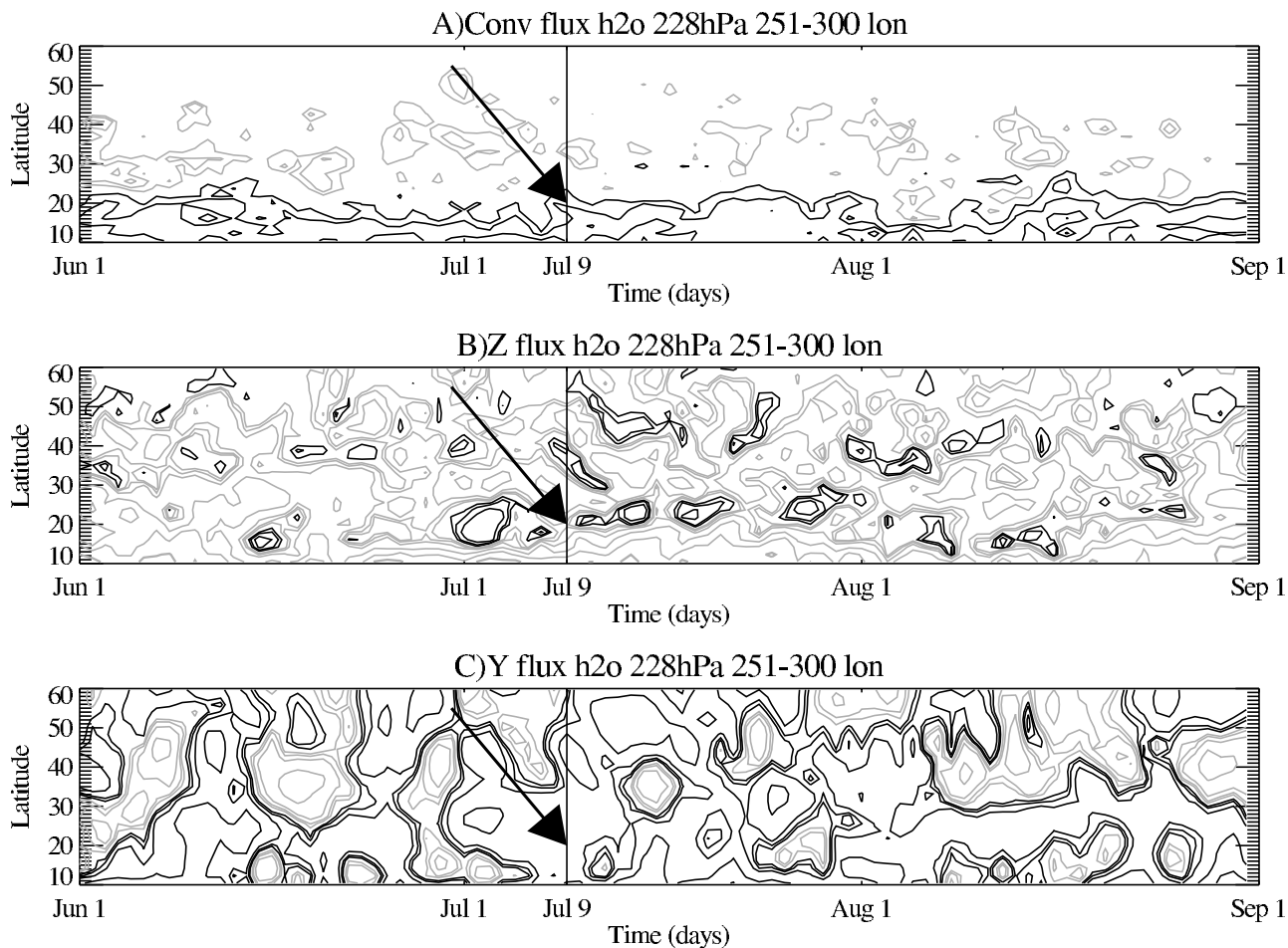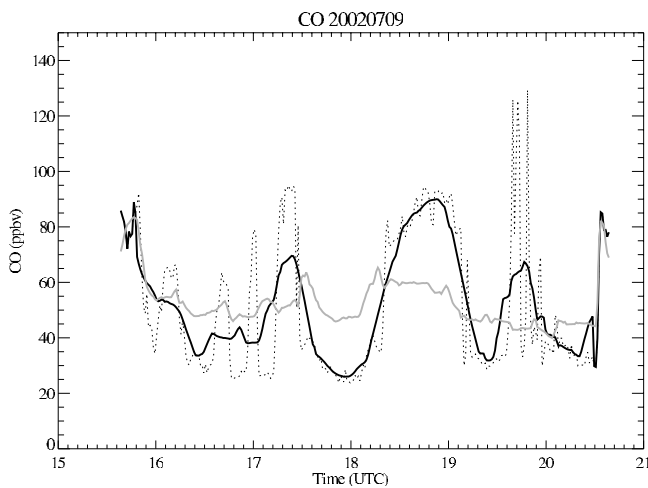
A) 709 H2O 113hPa

B) 709 O3 113hPa

Figure 8. Maps of daily averaged (a) water vapor and (b) ozone from the MOZART simulation driven by ECMWF winds for 9 July 2002 at 113 hPa. Contour interval is 1 ppmv for water vapor (Figure 8a) and 50–100 ppbv for ozone, as indicated. The gray line is the tropopause, identified by a contour of constant potential vorticity (2 PVU).

[23] Water vapor associated with this event in Figure 8 does not appear on subsequent days to enter the tropics directly, but seems to remain on the poleward side of the tropopause, even up to 100 hPa. This event happens to be the most significant seen in the CRYSTAL-FACE observations over North America, and is also the most significant event in the simulation during June–August (Figure 9).

A)Conv flux h2o 228hPa 251-300 lon

B)Z flux h2o 228hPa 251-300 lon

C)Y flux h2o 228hPa 251-300 lon

Figure 9. Water vapor mass flux from MOZART simulation at 228 hPa and averaged over 251–300 longitude. (a) Convective flux, (b) vertical (Z) flux, and (c) meridional (Y) flux. Upward and northward motion is in gray contours, and downward and southward motion is in black contours.

Figure 10. Observed (black dotted line) carbon monoxide concentrations along the flight track from CRYSTAL-FACE on 9 July 2002, and observations smoothed with a 200-km boxcar smoother (black solid line). The gray line indicates model simulation of CO interpolated to the flight track.

[24] This flux is partially convective, and partially in the simulated vertical fluxes. Convection in the simulation tails off rapidly above the tropopause. However, some of the vertical fluxes are also convective. The ECMWF analyses are implying more vertical motion than the model convection, and likely some of it is partitioned as a vertical mass flux, not as a convective flux.

[25] *Ray et al.* [2004] and *Richard et al.* [2003] have illustrated in detail using other tracers available during CRYSTAL-FACE that the source of this air is indeed convection at high latitudes. In particular, *Ray et al.* [2004] note that it is likely that the air can be traced back to boreal forest fires in eastern Canada. Figure 10 illustrates the observed and simulated carbon monoxide, a tracer of surface combustion processes, for the flight of 9 July. The location of the high-ozone tongue in Figure 4 is from 16−17 and 19.5−20 UTC of the flight, corresponding to the observed CO spikes and indicating high-ozone air associated with high water vapor and high CO. The model variability of CO is much less than observations, though large-scale variations in simulated CO are well correlated with observations if they are smoothed to approximately model resolution (~200 km). The model should not be expected to fully reproduce the range of CO observations, because individual source events such as specific fires are not present in the model, which instead has climatological mean sources. These fire events are an important possible source for the high CO found on this flight [*Ray et al.*, 2004].

[26] We have performed a similar analysis over the south Asia region. An examination of daily maps (similar to Figure 8) and meridional fluxes (similar to Figure 9c) for August to September 2002 indicates that high-ozone, high-water-vapor events from high latitudes to low latitudes are not seen over south Asia during this time period. High-latitude air generally stays well north of the tropopause, which is located further north at the same altitudes as over

North America. The result is the climatological picture from Figures 1 and 2. Higher ozone is found over North America, but with similar water vapor. Over Asia, ozone and water vapor have the same source, near surface air. Over North America, it appears that continental convection injects water vapor in the simulation well into the stratosphere, where it is advected to lower altitudes. *Ray et al.* [2004] have analyzed the observations from CRYSTAL-FACE and found that ~15% of the air along the flight track for 9 July between the 380-K and 390-K potential temperature surfaces is tropospheric air.
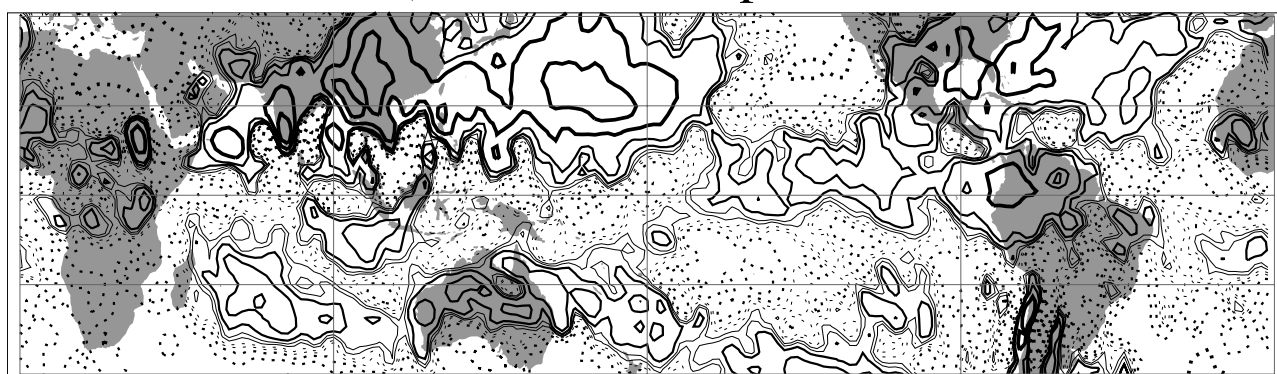
[27] Thus the O_3-H_2O correlations between the monsoon circulations are different because of a different origin of air masses, and different configurations of the boreal summer general circulation in the lowermost stratosphere. Over south Asia, the monsoon anticyclone isolates air within it, which is evident on the basis of streamlines [*Dunkerton*, 1995] or trajectory analyses (K. P. Bowman, personal communication, 2004). Over North America, the monsoon circulation is centered over the American Southwest and northern Mexico, and is not as isolated or as big. Significant quantities of high-latitude air move southward over eastern North America, and water vapor is added to this air mass by convection. A simple linear mixture of tropospheric air with low ozone and high water vapor, and stratospheric air with high ozone and low water vapor, can generate the anomalous correlations in Figure 6a. In the simulation, mixing air at the 420-K potential temperature surface (600−700-ppbv O_3 and 3-ppmv H_2O) with air from 340 K or below (100-ppbv O_3 and 50-ppmv H_2O) can generate the correlations. A similar result holds for the observations (Figure 6b), though potential temperatures below 350 K were not observed during cruise legs of the flight.

4. Simulated STE

[28] The simulations can also be used to better understand the exchange of air between the stratosphere and the troposphere during boreal summer. Given the fidelity of the model to observations illustrated in the previous section both on a climatological basis (Figures 1−3) as well as for detailed events (Figures 4−10), there is some confidence in examining the fluxes in the model where we do not have any observations, and drawing conclusions from these fluxes. For 2002, fluxes of ozone and water vapor from the simulation were totaled daily, and saved on the 3 dimensional model grid. The results indicate the model fluxes can reproduce many of the main known features of the annual cycle of stratosphere troposphere exchange, and allow a detailed look at the boreal summer season, particularly where observations do not exist.

[29] Several climatological features are illustrated in Figure 11. Figure 11a illustrates the simulated vertical flux of water vapor totaled over January−March 2002 in the simulation. The largest vertical flux is seen in the Southern Hemisphere over the central Pacific and South America. Similar upward motion is found north of the equator. Downward fluxes are concentrated over the eastern Pacific, especially in the subtropics. These motions are consistent with the Hadley and Walker circulations during this season. In Figure 11a there is a downward flux of water vapor over

A) 80hPa Jan-Mar Flux H2O
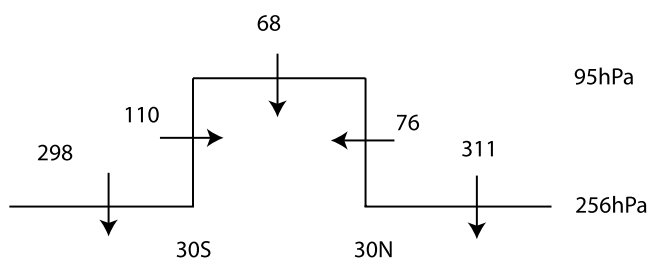

B) 80hPa Jul-Sep Flux H2O

Figure 11. Seasonal vertical flux of water vapor at 80 hPa for (a) January−March and (b) July−September. Upward fluxes are solid, and downward fluxes are dotted. Contour levels are $\pm 1 \times 10^7$ to 2.5×10^9 by decade (1, 2.5, 5) (in kg). Thicker contours are larger magnitudes.

the maritime continent (Indonesia), noted previously in observations [*Sherwood*, 2000] and simulations [*Gettelman et al.*, 2000; *Hatsushika and Yamazaki*, 2003]. *Hatsushika and Yamazaki* [2003], on the basis of GCM simulations, explain this downward flux as isentropic flow over downward pressure sloping isentropes, with reduction of longwave heating from deep convective anvils suppressing upward motion.
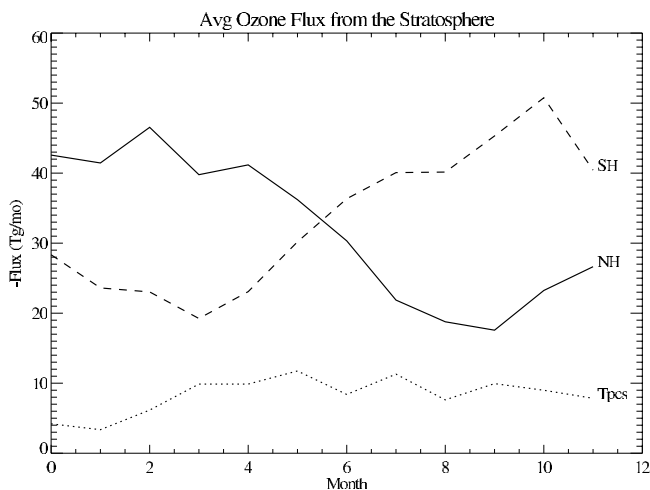
[30] During July−September (Figure 11b) the situation is vastly different. The largest fluxes of water vapor at 80 hPa are over Asia and the western Pacific, extending from South Asia to the dateline, at about 15°N. There are also significant upward fluxes of water vapor over eastern North America, and over the Atlantic at 20°N or so, consistent with the fluxes described in detail in the previous section. The two panels in Figure 11 echo the idea given by *Dunkerton* [1995] that the summer monsoon circulations in each hemisphere are not mirror images of each other. This is an important point since most observations have been concentrated in Northern Hemisphere winter, analyzing the situation in Figure 11a only.

[31] A qualitatively identical picture is evident for simulated ozone fluxes (not shown) in each season, but with correspondingly lower magnitude of the fluxes (due to ozone concentrations 1−2 orders of magnitude lower than water vapor).

[32] The total annual cross tropopause ozone flux is illustrated schematically in Figure 12. The flux is reported across pressure and latitude surfaces. The overall total flux of ozone into the troposphere of 863 Tg/yr is not strongly sensitive to the pressure surface or the latitude of the tropopause break chosen. The total flux of ozone across the tropopause is almost a factor of 2 higher than most estimates [*Horowitz et al.*, 2003], and nearly twice as large as the estimate from *Horowitz et al.* [2003] using the MOZART model and similar general circulation model winds to the WACCM winds used here (ozone fluxes were not available from the WACCM run). The discrepancy is likely due to spurious vertical transport in the ECMWF

Figure 12. Schematic annual total net ozone flux for 2002 in Tg yr^{-1}.

Figure 13. Monthly total ozone flux across the "tropopause" in Tg O_3 month^{-1}. Downward fluxes are positive, for the Northern Hemisphere (solid line), Southern Hemisphere (dashed line), and tropics (dotted line).

analysis system. This may occur because of slight systematic errors in the model physics relative to observations, resulting in spurious stratosphere-troposphere exchange [*Gettelman and Sobel*, 2000].

[33] However, Figure 13 indicates that the annual cycle of the ozone fluxes in each hemisphere (summing the meridional flux across the tropopause break) is coherent and reasonable, even if the magnitude of the total flux is high. The net ozone flux into the troposphere has a broad peak in each hemisphere from late winter to spring, and a consistent, small net downward flux in the tropics. Observations and other models indicate a larger ozone flux in the Northern Hemisphere [*Horowitz et al.*, 2003], though in the MOZART simulation with ECMWF winds the fluxes are nearly equal between hemispheres. On balance, the model driven by ECMWF winds broadly reproduces the annual cycle of ozone fluxes in the troposphere, with some
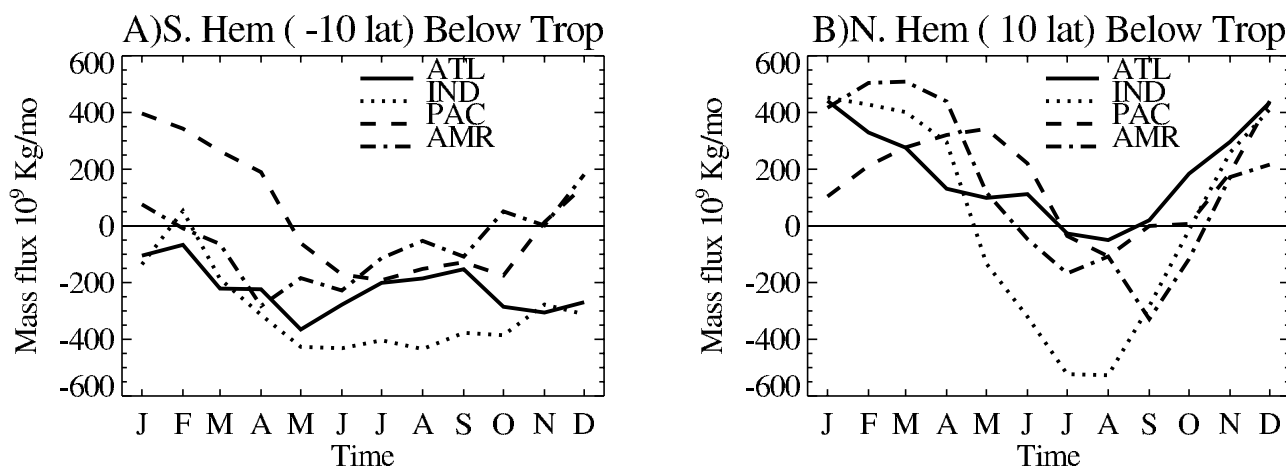
differences in magnitude which may be due to the nature of the analysis system. It is a good basis, however, on which to look at fluxes in more detail.

[34] Figure 14 illustrates the monthly total meridional flux of water vapor at 10°S (Figure 14a) and 10°N (Figure 14b) for four zonal regions of the tropics averaged for the upper troposphere below the tropical tropopause (256−113 hPa). These meridional fluxes represent air that is entering or leaving the "deep" tropics, and reveals details of the upward branch of the Hadley circulation, the mean meridional overturning circulation in the troposphere. The four zonal regions illustrated are as follows: the Atlantic region (ATL: 330°−60° longitude), the Indian Ocean and Asian region (IND: 60°−150°) the central Pacific (PAC: 150°−240°) and the American region (AMR: 240°−330°).
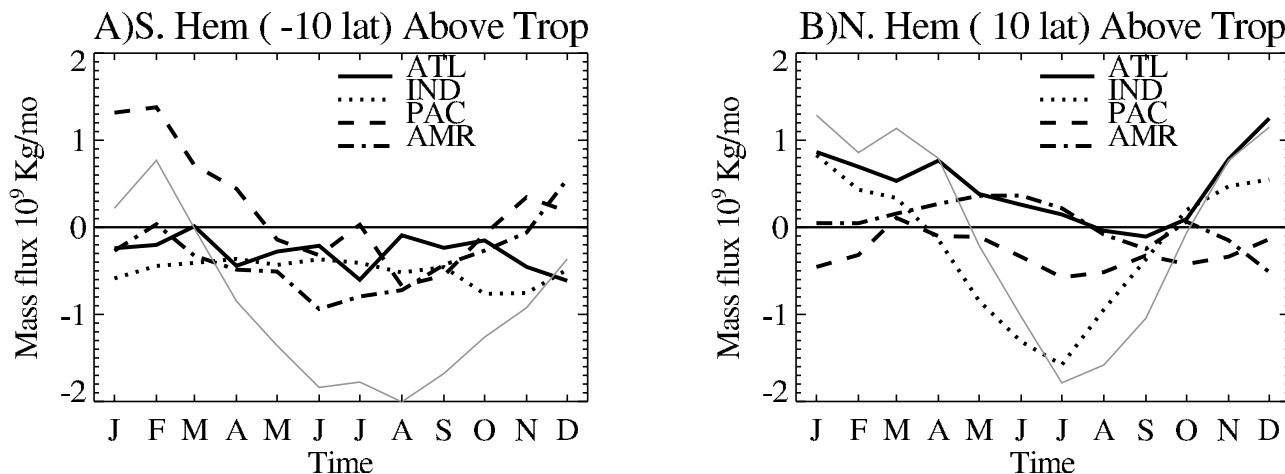
[35] Below the tropopause in the Southern Hemisphere (Figure 14a) there is a negative net meridional flux (toward the South Pole) all year round over the Atlantic and Indian regions. The net meridional fluxes are positive (equatorward in the Southern Hemisphere) in the Pacific and American sectors in boreal winter, consistent with the overturning branch of the Hadley cell. In the Northern Hemisphere (Figure 14b) fluxes are equatorward in the Indian and American regions in boreal summer.

[36] Following *Dunkerton* [1995], a local Hadley circulation can be defined in terms of the meridional motion averaged over a wide enough range of longitudes to encompass the rotational circulations associated with each of the major monsoon regions. These rotational circulations cancel when the (partial) zonal average is taken. It is mainly for this reason that we find (in several of the individual regions) a large, seasonally varying interhemispheric flux of water vapor in the upper troposphere (256−113 hPa) in the range of altitudes where the Hadley circulation outflow maximizes.

[37] The situation is different in the lower stratosphere (Figure 15), where the Hadley circulation appears only in global statistics (the thin gray line in Figure 15), except perhaps in the Indian sector during Northern Hemisphere summer (Figure 15b) and in the Pacific during Southern

Figure 14. Monthly meridional flux of water vapor by zonal region vertically averaged below the tropopause (256−113 hPa) across (a) 10°S and (b) 10°N.

A) S. Hem (-10 lat) Above Trop

B) N. Hem (10 lat) Above Trop

Figure 15. Monthly meridional flux of water vapor by zonal region vertically averaged above the tropopause (95–66 hPa) across (a) 10°S and (b) 10°N. Thin gray line is the zonal mean.

Hemisphere summer (Figure 15a). Elsewhere the numbers are smaller. In the Southern Hemisphere (Figure 15a) the Pacific region dominates the flux in Southern Hemisphere summer, consistent with flow into the tropics in this season. In the Northern Hemisphere (Figure 15b) it is the Indian region which dominates the equatorward flux in the Northern Hemisphere into the tropics above the tropopause.

[38] Lagrangian trajectory analyses are consistent with the Eulerian flux analysis above. We have examined an extensive set trajectories for June to August 2002 driven by analyses from the National Centers for Environmental Prediction (NCEP) (K. P. Bowman, personal communication, 2004). Trajectories over the South China Sea and the Philippines in the return flow of the Asian monsoon can reach the equator above the tropopause, having not crossed the tropical tropopause. This is consistent with return flow of the monsoon entering the tropics noted by *Bannister et al.* [2004] analyzed with GCM winds. It is also consistent with the trajectory analyses of *Fueglistaler et al.* [2004] using ECMWF analysis winds, which show that this region (as part of the "western Pacific") is responsible for a majority of the air entering the stratosphere in July and August. Thus flow around the tropical tropopause in the Asian monsoon is found regardless of the model or assimilation system used.

[39] Meridional ozone fluxes are similar to the water vapor fluxes described above. The only significant difference is a reversal of the ozone flux in the Northern Hemisphere below the tropopause, where the ozone flux is toward the equator in boreal winter, and the magnitude of the ozone flux into the tropics during boreal summer below the tropopause is more nearly equal between the monsoon circulations over the American and Indian sectors.

[40] A simple budget of July–September 2002 in the simulation driven by ECMWF winds indicates the importance of these different regions. The net vertical flux of water vapor over the Indian region (10°–30°N and 60°–150°E) from July–September is 75% of the total net tropical (±30) flux of water vapor at 95 hPa, and 54% at 66 hPa. The region represents approximately 8% of the
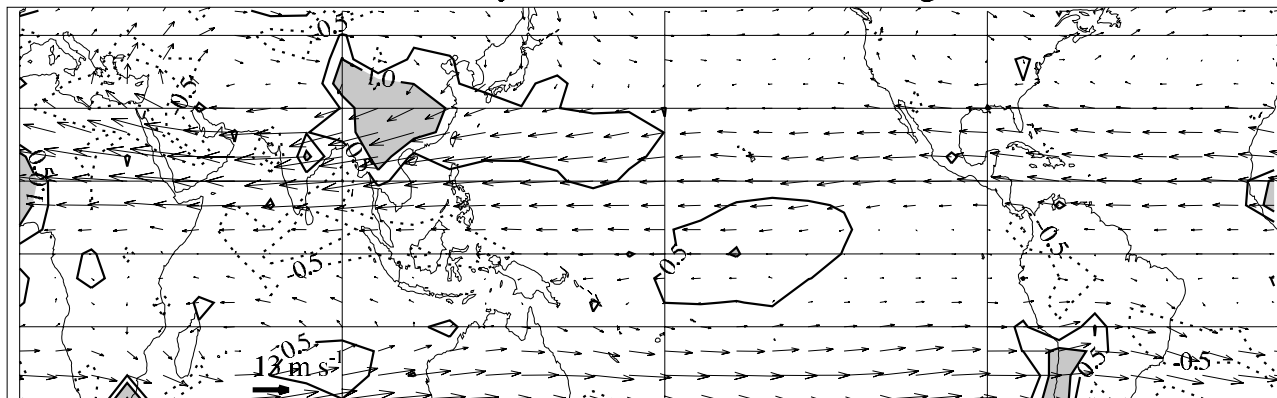
area of the tropics. The vertical flux of water vapor over North America (10°–30°N and 240°–330°E) is 7% of the total tropical upward flux at 95 hPa, and 18% at 66 hPa. While simulated water vapor (Figure 2) is higher than observed water vapor (Figure 1), the gradients are similar and the maximum over south Asia is ~20% larger in both, thus the ratio of regional fluxes to total is probably a better statistic here than absolute magnitudes. These ratios are similar to simulations by *Bannister et al.* [2004], who indicate that at least 25% of the water vapor concentration at 30 hPa comes from the Asian monsoon, though they use a smaller area (6% of the tropics), and the numbers are not directly comparable (one is a flux, and the other is a concentration). The monsoon transport over Asia dominates the simulated upward tropical flux well into the stratosphere, though the fluxes are more zonally symmetric at 66 hPa. Ozone fluxes are net downward in this region and are not as good a tracer of vertical transport.

[41] Examination of model fluxes over the 22-year model run indicates large interannual variability of water vapor and ozone fluxes in July–September. Given 22 realizations of the boreal summer flux, there is no trend that is significantly different from the large interannual variability. This does not preclude the possibility that changes in the monsoon can contribute to water vapor trends, since the model may not properly represent the intraseasonal variability of the monsoon.
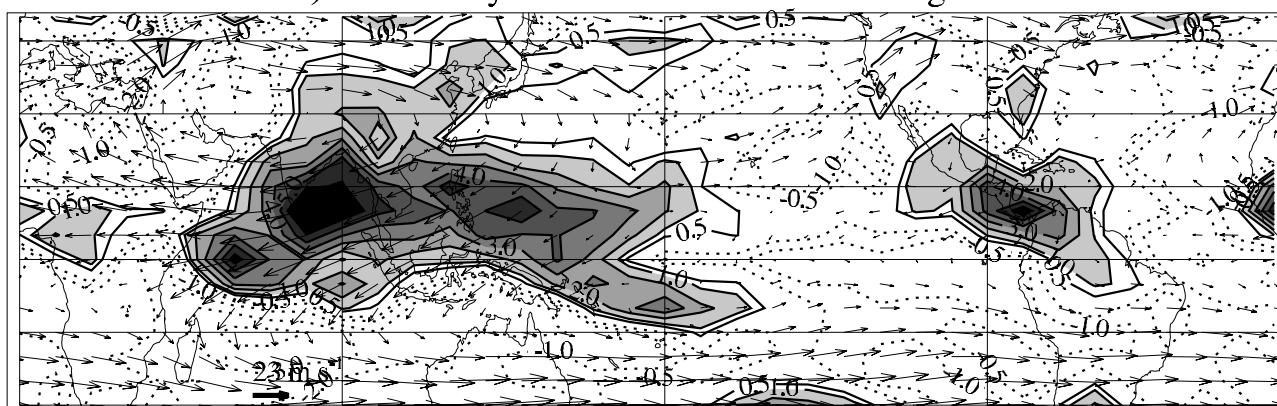
[42] The conceptual framework for stratosphere-troposphere exchange in the tropics starts with large regions of cloud-scale convection. This convection locally mixes air and humidity across potential temperature (isentropic) surfaces. The mixing may be well off the equator. Large-scale motions subsequently redistribute the moist air across the tropics, and the air may rise to higher potential temperature surfaces through heating in the course of these circulations, spiraling upward. Some of these isentropic surfaces may lie above the cold point tropopause. The large-scale circulation itself is strongly affected by the distribution of convective heating [*Gill*, 1980]. The framework is well illustrated in Figure 16b, showing the July climatological (from NCEP/

A) Jul Monthly Mean 70hPa Wind & Divergence

B) Jul Monthly Mean 150hPa Wind & Divergence

Figure 16. July mean vector wind (arrows) and divergence in 1×10^{-6} s^{-1} for (a) 70 hPa and (b) 150 hPa. Data are from NCEP/NCAR reanalyses [*Kalnay et al.*, 1996].

NCAR reanalyses) wind and divergence (shaded) at 150 hPa. The anticyclone over Asia entrains air rising from below (divergence at upper levels is associated with upward motions), circulates it around the anticyclone, and it may enter the tropics at higher levels, where there is still divergence up to 70 hPa on the return flow into the tropics (Figure 16a). The American monsoon is not as large a feature, and not as isolated, the climatological wind pattern matching well the ridging in the ozone distribution in Figures 1 and 2. It is also important to note that the moist Hadley and Walker circulations which dominate the divergence at 150 hPa (Figure 16b) do not penetrate strongly into the stratosphere (Figure 16a), but that the rotational circulations of the monsoon anticyclones do penetrate the stratosphere, and can cause mixing of moist air back into the tropics.

5. Conclusions

[43] The simulations using MOZART forced with ECMWF winds for the period of the CRYSTAL-FACE observations indicate that the MOZART CTM is good at representing observed transport events. The high ozone observed up to 400 K during the 9 July 2002 flight of the WB57 appears to come from high latitudes, as indicated in previous analysis [*Richard et al.*, 2003]. The higher water

vapor also observed in this air mass appears to have a high-latitude convective origin in the simulations, as postulated by *Ray et al.* [2004]. This is in addition to model vertical fluxes with appear to loft air well above the tropopause in midlatitudes.

[44] This feature appears to be present in the simulated climatology of ozone and water vapor in the summertime lowermost stratosphere. A climatology of ozone and water vapor from a long CTM run agrees well with the observed satellite climatology. This is true over North America, as well as over south Asia, where in situ observations of water vapor and ozone are not available. The differences in water vapor and ozone between these regions are due to large-scale transport and the difference between the monsoon circulations.

[45] The North American monsoon is smaller, does not reach well into the stratosphere, and is not an isolated circulation, but rather appears to draw air up from the tropics on the west side, and from high latitudes on the east side. This circulation may entrain air from the high-latitude troposphere, even near the surface, and loft it into the subtropical lower stratosphere. However, there is little evidence of this air crossing into the deep tropics (equatorward of 10°N) in the simulation over North America, in a time series of plots similar to Figure 8, which corroborates the limited meridional flux into the tropics in Figure 14,

except in September. Over south Asia the core of the monsoon anticyclone is more isolated, but leads to large equatorward meridional transport.

[46] Given the fidelity of the model for these specific and climatological events, we use detailed fluxes to examine transport in the upper troposphere and lower stratosphere in regions beyond those observed during CRYSTAL-FACE. Simulated ozone fluxes are high relative to observations, but have an appropriate seasonal cycle. The seasonal cycle of water vapor fluxes in the lower stratosphere during Northern Hemisphere summer is vastly different from that during the winter season. Monsoon fluxes in the Northern Hemisphere play a major role in this planetary-scale circulation, which fits into a conceptual framework of how air enters the stratosphere in boreal summer.

[47] The Indian region (including the equatorward branch of the Asian monsoon anticyclone over the western Pacific) outside of the deep tropics is responsible for nearly 3/4 of the net tropical upward flux of water vapor during July–September at 95 hPa, and over half at 66 hPa in the simulation. The meridional fluxes also show significant transport of this air into the deep tropics, both below and above the tropopause. This transport into the tropics in the simulation appears to bypass the cold point tropopause, consistent with observed climatological flow. Observations of water vapor from HALOE do not show similar clear transport of air into the tropical lower stratosphere around the tropical tropopause. However, there may exist a dry bias in HALOE, especially below the tropopause, because HALOE cannot retrieve in the presence of clouds, and the Asian monsoon region is one of the regions with the highest frequency of convective clouds at and above the tropopause [*Gettelman et al.*, 2002].

[48] The results of the simulation indicate that monsoon air can bypass the tropical tropopause, and enter the stratosphere in the subtropics ($10°–30°N$ in boreal summer). Some of this air enters the tropics above the tropopause, and can be lofted into the stratosphere. Observations do not clearly indicate this as a pathway for transport, but are of insufficient resolution to resolve this transport. Such a result, if confirmed, would indicate a pathway for water vapor to enter the stratosphere without passing through the region of cold tropical tropopause temperatures. This might have a significant impact on water vapor trends. Model simulations do not show any trends in the monsoon flux of water vapor in a 22-year simulation, but the interannual variability is high.

[49] Confirmation of this transport pathway with better observations should be possible in the near future with new satellite observations in the upper troposphere and lower stratosphere expected from the MLS and HIRDLS instruments on the Aura satellite. Additional validation with in situ observations over monsoon regions, particularly the Asian monsoon, may be critical for understanding the transport of humidity into the stratosphere.

References

Bannister, R. N., A. O'Neill, A. R. Gregory, and K. M. Nissen (2004), The role of the South-East Asian monsoon and other seasonal features in creating the 'tape recorder' signal in the unified model, *Q. J. R. Meteorol. Soc.*, 130, 1531–1554, doi:10.1256/qj.03.106.

Dunkerton, T. J. (1995), Evidence of meridional motion in the summer lower stratosphere adjacent to monsoon regions, *J. Geophys. Res.*, 100, 16,675–16,688.

Friedl, R. R. (Ed.) (1997), Atmospheric effects of subsonic aircraft: Interim assessment report of the Advanced Subsonic Technology Program, *NASA Ref. Publ., 1400*.

Fueglistaler, S., H. Wernli, and T. Peter (2004), Tropical troposphere-to-stratosphere transport inferred from trajectory calculations, *J. Geophys. Res.*, 109, D03108, doi:10.1029/2003JD004069.

Gettelman, A., and A. H. Sobel (2000), Direct diagnoses of stratosphere-troposphere exchange, *J. Atmos. Sci.*, 57, 3–16.

Gettelman, A., A. R. Douglass, and J. R. Holton (2000), Simulations of water vapor in the upper troposphere and lower stratosphere, *J. Geophys. Res.*, 105, 9003–9023.

Gettelman, A., M. L. Salby, and F. Sassi (2002), Distribution and influence of convection in the tropical tropopause region, *J. Geophys. Res.*, 107(D10), 4080, doi:10.1029/2001JD001048.

Gill, A. E. (1980), Some simple solutions for heat-induced tropical circulation, *Q. J. R. Meteorol. Soc.*, 106, 447–462.

Hatsushika, H., and K. Yamazaki (2003), Stratospheric drain over Indonesia and dehydration within the tropical tropopause layer diagnosed by air parcel trajectories, *J. Geophys. Res.*, 108(D19), 4610, doi:10.1029/2002JD002986.

Horowitz, L. W., et al. (2003), A global simulation of tropospheric ozone and related tracers: Description and evaluation of MOZART, version 2, *J. Geophys. Res.*, 108(D24), 4784, doi:10.1029/2002JD002853.

Kalnay, E., et al. (1996), The NCEP/NCAR 40-year reanalysis project, *Bull. Am. Meteorol. Soc.*, 77(3), 437–471.

Lin, S. J., and R. B. Rood (1996), Multidimensional flux-form semi-Lagrangian transport schemes, *Mon. Weather Rev.*, 124(9), 2046–2070.

McCormick, M. P., J. M. Zawodny, R. E. Viega, J. C. Larsen, and P. H. Wang (1989), An overview of SAGE I and II ozone measurements, *Planet. Space Sci.*, 37, 1567–1586.

Mote, P. W., et al. (1996), An atmospheric tape recorder: The imprint of tropical tropopause temperatures on stratospheric water vapor, *J. Geophys. Res.*, 101, 3989–4006.

Park, M., W. J. Randel, D. E. Kinnison, R. R. Garcia, and W. Choi (2004), Seasonal variation of methane, water vapor, and nitrogen oxides near the tropopause: Satellite observations and model simulations, *J. Geophys. Res.*, 109, D03302, doi:10.1029/2003JD003706.

Pickering, K., Y. Wang, W. K. Tao, C. Price, and J. Mueller (1998), Vertical distributions of lightning NO_x for use in regional and global chemical transport models, *J. Geophys. Res.*, 103, 31,203–31,216.

Podolske, J., and M. Loewenstein (1993), Airborne tunable diode laser spectrometer for trace-gas measurement in the lower stratosphere, *Appl. Opt.*, 32, 5324–5333.

Price, C., J. Penner, and M. Prather (1997), NO_x from lightning: 1. Global distribution based on lightning physics, *J. Geophys. Res.*, 102, 5929–5941.

Proffitt, M. H., and R. L. McLaughlin (1983), Fast-response dual-beam uv-absorption ozone photometer suitable for use in stratospheric balloons, *Rev. Sci. Instrum.*, 54, 1719–1728.

Randel, W. J., F. Wu, R. Swinbank, J. Nash, and A. O'Neill (1999), Global QBO circulation derived from UKMO analyses, *J. Atmos. Sci.*, 56, 457–474.

Randel, W. J., A. Gettelman, F. Wu, J. M. Russell III, J. Zawodny, and S. Oltmans (2001), Seasonal variation of water vapor in the lower stratosphere observed in Halogen Occultation Experiment data, *J. Geophys. Res.*, 106, 14,313–14,325.

Randel, W. J., F. Wu, S. J. Oltmans, K. Rosenlof, and G. E. Nedoluha (2004), Interannual changes of stratospheric water vapor and correlations with tropical tropopause temperatures, *J. Atmos. Sci.*, 61, 2133–2148.

Rasch, P. J., N. W. Mahowald, and B. E. Eaton (1997), Representations of transport, convection, and the hydrologic cycle in chemical transport models: Implications for the modeling of short-lived and soluble species, *J. Geophys. Res.*, 102, 28,127–28,138.

Ray, E. A., et al. (2004), Evidence of the effect of summertime midlatitude convection on the subtropical lower stratosphere from CRYSTAL-FACE tracer measurements, *J. Geophys. Res.*, 109, D18304, doi:10.1029/2004JD004655.

Richard, E. C., K. C. Aikin, E. A. Ray, K. H. Rosenlof, T. L. Thompson, A. Weinheimer, D. Montzka, D. Knapp, B. Ridley, and A. Gettelman (2003), Large-scale equatorward transport of ozone in the subtropical lower stratosphere, *J. Geophys. Res.*, 108(D23), 4714, doi:10.1029/2003JD003884.

Sassi, F., D. Kinnison, B. A. Boville, R. R. Garcia, and R. Roble (2004), Effect of El Niño-Southern Oscillation on the dynamical, thermal, and chemical structure of the middle atmosphere, *J. Geophys. Res.*, *109*, D17108, doi:10.1029/2003JD004434.

Sherwood, S. C. (2000), A stratospheric "drain" over the maritime continent, *Geophys. Res. Lett.*, *27*(5), 677–680.

Smith, C. A., R. Toumi, and J. D. Haigh (2000), Seasonal trends in stratospheric water vapour, *Geophys. Res. Lett.*, *27*(12), 1687–1690.

Webster, P. J., V. O. Magana, T. N. Palmer, J. Shukla, R. A. Thomas, M. Yanai, and T. Yasunari (1998), Monsoons: Processes, predictability and the prospects for prediction, *J. Geophys. Res.*, *103*, 14,451–14,510.

Weinstock, E. M., et al. (1994), New fast response photofragment fluorescence hygrometer for use on the NASA ER-2 and the Perseus remotely piloted aircraft, *Rev. Sci. Instrum.*, *65*, 3544–3554.

Yulaeva, E., J. R. Holton, and J. M. Wallace (1994), On the cause of the annual cycle in tropical lower-stratospheric temperatures, *J. Atmos. Sci.*, *51*, 169–174.

―――――――――――

G. P. Brasseur, A. Gettelman, and D. E. Kinnison, National Center for Atmospheric Research, Box 3000, Boulder, CO 80307-3000, USA. (andrew@ucar.edu)

T. J. Dunkerton, Northwest Research Associates, 14508 N.E. 20th Street, Bellevue, WA 98007-3713, USA.